

Milky Way Globular Clusters: close encounter rates with each other and with the Central Supermassive Black Hole

M. V. Ishchenko^{1*}, M. O. Sobolenko¹, M. T. Kalambay^{2,3,4}, B. T. Shukirgaliyev^{4,3}, P. P. Berczik^{5,1}

¹Main Astronomical Observatory, National Academy of Sciences of Ukraine,
27 Akademika Zabolotnoho St., 03143, Kyiv, Ukraine

²Al-Farabi Kazakh National University, 71 Al-Farabi Av., 050040 Almaty, Kazakhstan
20A Datun Rd., Chaoyang District, 100101 Beijing, China

³Fesenkov Astrophysical Institute, 23 Observatory St., 050020 Almaty, Kazakhstan

⁴Energetic Cosmos Laboratory, Nazarbayev University, 52 Kabanbay Batyr Av., 010000 Nur-Sultan, Kazakhstan

⁵National Astronomical Observatories and Key Laboratory of Computational Astrophysics, Chinese Academy of Sciences,
20A Datun Rd., Chaoyang District, Beijing 100101, China

Using the data from *Gaia* (ESA) Data Release 2 we performed the orbital calculations of globular clusters (GCs) of the Milky Way. To explore possible collisions between the GCs, using our developed high-order φ -GRAPE code, we integrated (backwards and forward) the orbits of 119 objects with reliable positions and proper motions. In calculations, we adopted a realistic axisymmetric Galactic potential (*bulge + disk + halo*). Using different impact conditions, we found three pairs of the GCs that likely experienced collisions: Terzan 3 – NGC 6553, Terzan 3 – NGC 6218, Liller 1 – NGC 6522, Djorg 2 – NGC 6552 and NGC 6355 – NGC 6637.

We analyzed the GCs interaction rates with the central supermassive black hole. Assuming the maximum 100 pc distance criteria for separation between them we estimated 11 close encounter events. From our numerical simulations we estimate the close interaction rate as: at least one event per Gyr with the impact parameter less than 30 pc; and one event per Myr with the impact parameter less than 60 pc. Our calculations show one very close encounter of NGC 6121 with the central SMBH near 5.5 pc (practically direct collision). Based on the extended literature search for the possible progenitor of our selected 11 GCs, we found that most of them have a Milky Way main bulge origin.

Key words: Galaxy: globular clusters, supermassive black hole: general - Galaxy: kinematics and dynamics - methods: numerical

INTRODUCTION

The globular clusters (GCs) of the Milky Way (MW) are old gravitationally bound stellar systems with typical ages older than 6 Gyr and masses $\gtrsim 10^4 M_\odot$ [16]. These objects can be used as a powerful tool to examine the Galactic structure and assembly the history at different scales from the formation of star clusters to hierarchical merger events [17]. The recent high precision astrometric measurements provided by *Gaia* Data Release 2 (DR2) [10] allows us to calculate the mean proper motions for ≈ 150 GCs of the MW [6, 10, 28]. In this work, by using two catalogues of GCs [6, 28] containing the full 6D phase-space information, we performed the simulations of 148 GCs orbits aiming to test a possibility of the GCs collisions in the past 5 Gyr. Similar to previous studies, we study the dynamics of the GCs as the test-particle motion in axisymmetric MW-like

potential [1, 2, 12, 21, 23–25].

GLOBULAR CLUSTER SAMPLE

Prior to the orbital integration, we prepared a complete catalogue of the MW GCs. That is, we merged two recent catalogues [6, 28] which together contain the information about 152 objects (see Table 4). The resulting catalogue contains the complete phase-space information required for the initial conditions in our simulations: right ascension (RA), declination (DEC) and distance (D), proper motions $\mu_{\alpha*} = \mu_\alpha \cos \delta$, μ_δ and radial velocity v_r .

To avoid the calculation of the GCs orbits with large uncertainties in initial conditions we have analysed the errors of the *Gaia* measurement. In Fig. 1 we show the relative errors for the radial velocity and proper motions where each GC has its own index

*marina@mao.kiev.ua

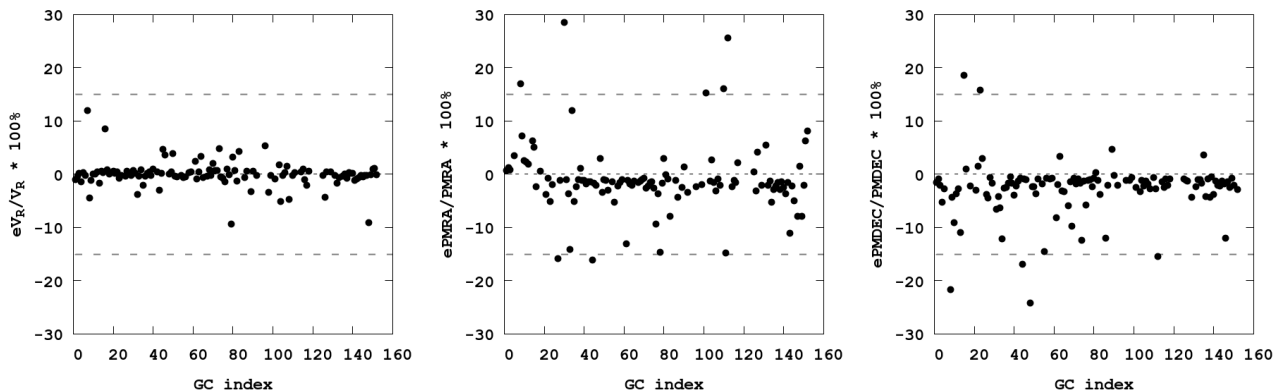


Fig. 1: Distribution of the GCs measurement errors for radial velocity v_r (left) and proper motions in right ascension (μ_{α^*} , center) and in declination (μ_{δ} , right). Dashed grey horizontal lines indicate 15% confidence range.

(see Table 4). Thanks to the precise *Gaia* measurements the uncertainties for the radial velocity (v_r) are quite small (mostly below 15%). However, as it is seen, for proper motions (μ_{α^*} , μ_{δ}) the situation is different. Therefore, we discard from our catalogue the GCs with the relative error larger than 30% for radial velocity and proper motions. We found that only 8 GCs do not satisfy our selection and in Table 4 these objects are marked with *me* (measurement error).

For calculating positions and velocities in the Galactocentric rest-frame (for basic coordinate transformation see [15]), we assumed an in-plane distance of the Sun from the Galactic centre of $X_{\odot}=8.178$ kpc [11] and $Z_{\odot}=20.8$ pc, a velocity of the Local Standard of Rest (LSR), $V_{\text{LSR}}=234.737$ km s $^{-1}$ [18], and a peculiar velocity of the Sun with respect to the LSR, $U_{\odot}=11.1$ km s $^{-1}$, $V_{\odot}=12.24$ km s $^{-1}$, $W_{\odot}=7.25$ km s $^{-1}$ [26].

ORBITS INTEGRATION

For the GCs orbit integration we adopted the MW-like gravitational potential based on the superposition of *bulge + disk + halo* models. In particular, the total potential consisting in a spherical bulge $\Phi_b(R, z)$, an axisymmetric disk $\Phi_d(R, z)$ and a spherical dark-matter halo $\Phi_h(R, z)$ can be written as follows:

$$\Phi(R, z) = \Phi_b(R, z) + \Phi_d(R, z) + \Phi_h(R, z), \quad (1)$$

where $R^2 = x^2 + y^2$ is the Galactocentric distance in polar coordinates and z is the vertical coordinate perpendicular to the disk plane.

Potentials of the bulge and the disk were taken in the form of Miyamoto-Nagai [20], while the dark matter potential is assumed to be Navarro-Frenk-

White (NFW) [22]:

$$\left\{ \begin{array}{l} \Phi_b(R, z) = -\frac{M_b}{(r^2 + b_b^2)^{1/2}}, \quad (2) \\ \Phi_d(R, z) = -\frac{M_d}{\left[R^2 + \left(a_d + \sqrt{z^2 + b_d^2} \right)^2 \right]^{1/2}}, \quad (3) \\ \Phi_h(R, z) = -\frac{M_h}{r} \ln \left(1 + \frac{r}{b_h} \right), \quad (4) \end{array} \right.$$

where $r = \sqrt{R^2 + z^2}$ is the spherical galactocentric distance. The values of masses and the scaling parameters of components can be found in Table 1 [3,4].

For the GCs orbital integration we used a high-order parallel dynamical N -body code φ -GRAPE which is based on the fourth-order Hermite integration scheme with hierarchical individual block time steps scheme [8]. More details about the code architecture and special GRAPE hardware can be found in [13].

Table 1: Galactic potential parameters.

Parameter	Value	Unit
Bulge mass M_b	1.03×10^{10}	M_{\odot}
Disk mass M_d	6.51×10^{10}	M_{\odot}
Halo mass M_h	29.00×10^{10}	M_{\odot}
Bulge scale param. b_b	0.2672	kpc
Disk scale param. a_d	4.4	kpc
Disk scale param. b_d	0.3084	kpc
Halo scale param. b_h	7.7	kpc

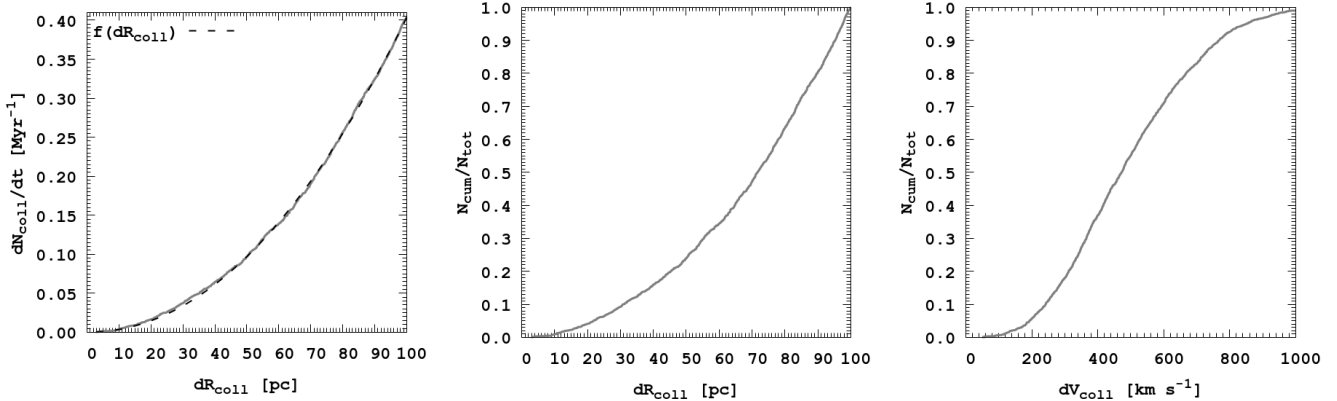


Fig. 2: GCs collision rate as a function of the relative distance (left), where black dashed line is a power-law fit (see equation 5). The normalized number of collisions as a function of the relative distance and relative velocity are shown in center and right panels, respectively.

GC COLLISION PAIRS

Before moving forward in the analysis of the collisions of the GCs population we have tested our numerical setup in order to keep tracking the GCs which orbits are the same during backward and forward integration. First, we integrated all 152 GCs backwards for 5 Gyr then we use the positions and velocities of all the GCs at the end of the simulations and integrate them forward for 5 Gyr. One could expect that the resulting positions and velocities should be identical to the observed ones. However, we have found that the orbits of 25 GCs are not invertible. These GCs usually pass by very close to the galactic center and most likely even an adaptive time-step is not able to capture their motions in the very center. Another possibility is a non-integrability of the potential which is hard to quantify and we leave this issue for further studies. Therefore, our final sample consists of 119 objects [9].

In order to count the number of collisions between pairs of GCs we used a set of three criteria. At the same time (i) a minimum separation between the GCs dR_{coll} should be <100 pc, (ii) the distance between the GCs should be less as twice of the sum of half-mass radii: $dR_{\text{coll}} < 2(R_{\text{hm},i} + R_{\text{hm},j})$ and (iii) the relative velocity between objects dV_{coll} should be: <200 km s $^{-1}$.

According to the first criteria we have 2019 and 1973 collisions during backward and forward orbits integration, respectively. The second condition reduces these numbers to 38 collisions. Finally, applying the last condition we obtained only five reliable collision events. In Table 2 we show the characteristics of GC collisional pairs for reliable collisions (Terzan 3 – NGC 6553, Terzan 3 – NGC 6218, Liller 1 – NGC 6522, Djorg 2 – NGC 6553, NGC 6355 – NGC 6637). It is worth mentioning, that all the

colliding GCs were likely formed in the MW disk [17].

Table 2: Characteristics of GC collisional pairs.

GC 1	GC 2	dR_{coll} (pc)	dV_{coll} (km s $^{-1}$)	Time (Myr)
Terzan 3	NGC 6553	25.58	148.18	237
Terzan 3	NGC 6218	10.75	183.12	581
Liller 1	NGC 6522	9.38	185.04	2625
Djorg 2	NGC 6553	20.22	153.14	2890
NGC 6355	NGC 6637	11.10	184.17	4886

In order to estimate the global collision rate, in Fig. 2 (left) we show the number of collisions per Myr as a function of impact parameter dR_{coll} . The distribution can be well fitted by a simple power-law function:

$$\frac{dN_{\text{coll}}}{dt} = 10^{a \cdot \lg(dR_{\text{coll}}) + b}, \quad (5)$$

where $a = 2.057 \pm 0.001$ and $b = -4.508 \pm 0.003$ are the fitting slope parameters. Therefore, we conclude that in each ten million years there is at least one collision with the impact parameter less than 50 pc.

In Fig. 2 we also present the normalized cumulative collisions number as a function of GC minimum impact parameter (center) and relative velocity at the moment of collision (right). As we can see the cumulative collision numbers can be also described by a power-law function, where the minimum values are $dR_{\text{coll}} \approx 3$ pc and $dV_{\text{coll}} \approx 85$ km s $^{-1}$.

INTERACTION RATES WITH CENTRAL SUPERMASSIVE BLACK HOLE

In order to count a number of interactions with a central Supermassive Black Hole (SMBH) of GCs,

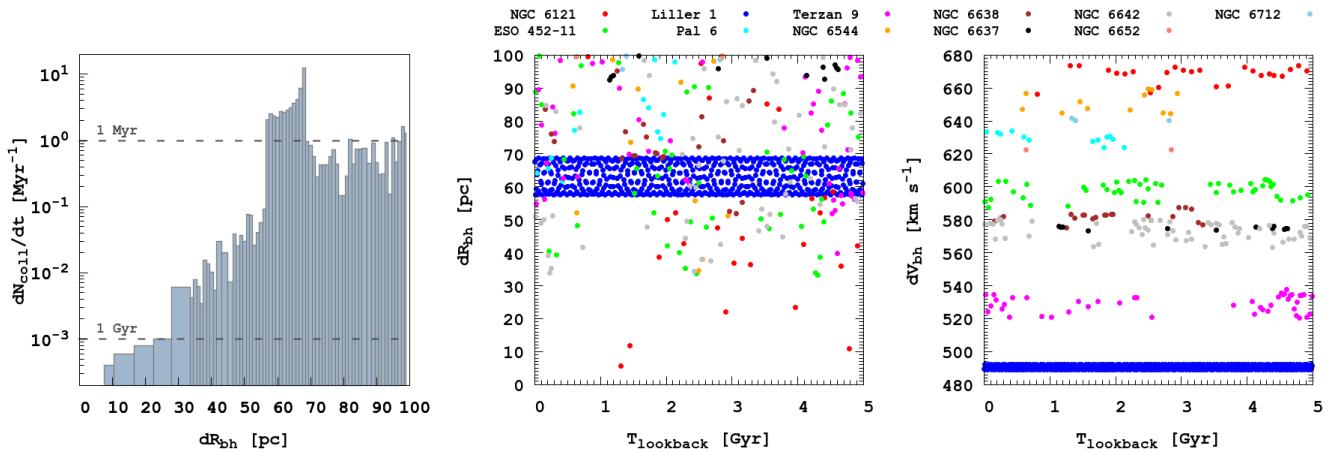


Fig. 3: Interaction rate of GCs with central SMBH (left), where grey dashed lines are levels of the one event per Gyr and one event per Myr. The impact parameter from the center (middle) and the orbital velocity (right) of the GCs are shown.

we used criteria of minimum separation between the GC and central SMBH dR_{bh} should be < 100 pc. In order to estimate the interaction rate of GC with central SMBH, in Fig. 3 (left) we show the number of events rate per Myr as a function of GC impact parameter dR_{bh} . According to this figure we can estimate the close interaction rate as one event per Gyr with the impact parameter less than 30 pc. Also we can conclude that we have at least one event per Myr with the impact parameter less than 60 pc.

According to the above criteria we can estimate 11 very close encounter events: NGC 6121, ESO 452-11, Liller 1, Pal 6, Terzan 9, NGC 6544, NGC 6638, NGC 6637, NGC 6642, NGC 6652 and NGC 6712. All of them have a very close passing orbit trajectory and a high probability of interaction with Milky Way SMBH. In Fig. 3 (center and right panels) we show the impact parameter from the center and the orbital velocity of the actual GCs. Each of the above 11 events is marked by different colors. As we can see from these panels the GC Liller 1 during the last five Gyr always have a close pericenter passage at a level of around 65 pc (blue points). The closest encounter with the central SMBH in our simulation has a 5.5 pc. This is the NGC 6121 GC (red points). The relatively high velocities can be easily explained by the strong dynamical influence of the SMBH on the orbital motion of GCs.

In Table 3 we present the interaction events of GCs with minimum separation (second column) from SMBH. On the third column we show the corresponding pericenter passage velocity and the time past when this event happens (fourth column). After the extended literature search we try to identify the GCs possible progenitors. In most cases the clusters have an MW main bulge origin.

Table 3: Characteristics of GCs that have closing pass with the central supermassive black hole.

GC	$dR_{\text{bh},\text{min}}$ (pc)	dV_{bh} (km s $^{-1}$)	Time (Myr)	Progenitor
NGC 6121	5.5	673	1314	Kraken [17]
ESO 452-11	33	604	4303	–
Liller 1	58	499	1859	XXX [19] MW [5]
Pal 6	62	634	427	LE [19] MB [27]
Terzan 9	40	637	4599	MB [19]
NGC 6544	35	569	2499	Kraken [17]
NGC 6638	52	587	3060	MB [19]
NGC 6637	92	575	1136	MB [19]
NGC 6642	34	580	2243	MB [19]
NGC 6652	99	622	640	MB [19]
NGC 6712	96	641	1330	LE [19] Kraken [17]

NOTE: Column Progenitor contains possible GC's origin with reference: Kraken - GC stands to Kraken accretion event, XXX - GC does not have available kinematics, LE - GC stands to the unassociated low-energy group, MB - GC stands to the main bulge, MW - GC stands to the *in situ* formation.

The detail interaction of the selected 11 GCs with the central SMBH we present in Fig. 4 - Fig. 9. The upper figures for each objects show's the global view of object trajectories. The bottom figures show's the detailed view of encounters. As we can see from the detailed visualization the GCs during the five Gyr of integration the GCs came to the central SMBH quite

often. On the summary Table 4 we present all the 152 globular clusters with full information about the clusters. As we can note the Liller 1 GC have both collisions with other cluster and also close interaction with central SMBH.

CONCLUSIONS

Using the present-day *Gaia* DR 2-based catalogues [6, 28] we have analyzed the orbits of the Milky Way globular clusters. From 152 GCs we discard 8 objects with large velocity errors. For the remaining 146 GCs, we analyse both backward and forward orbits calculated in the MW-like external potential using our developed high order φ -GRAPE code. Using complex criteria for the collisions detection we robustly identified five colliding pairs: Terzan 3 – NGC 6553, Terzan 3 – NGC 6218, Liller 1 – NGC 6522, Djorg 2 – NGC 6553, NGC 6355 – NGC 6637. We also estimated the overall collision rate as about one collision with the impact parameter less than 50 pc per 10 Myr.

Also we analyzed the GCs interaction rates with the central supermassive black hole. Assuming the maximum 100 pc distance criteria for separation between them we estimated 11 close encounter events: NGC 6121, ESO 452-11, Liller 1, Pal 6, Terzan 9, NGC 6544, NGC 6638, NGC 6637, NGC 6642, NGC 6652 and NGC 6712. From our numerical simulations we estimate the close interaction rate as: at least one event per Gyr with the impact parameter less than 30 pc; and one event per Myr with the impact parameter less than 60 pc. Our calculations show one very close encounter of NGC 6121 with the central SMBH near 5.5 pc (practically direct collision). Based on the extended literature search for the possible progenitor of our selected 11 GCs, we found that most of them have a Milky Way main bulge origin.

ACKNOWLEDGEMENT

The work of MI and MS was supported by the National Academy of Sciences of Ukraine under research project of young scientists No. 0121U111799. The work of MK and BS has been funded by the Science Committee of the Ministry of Education and Science of the Republic of Kazakhstan (Grant No. AP08856149, AP08856184 and BR10965141). PB acknowledges support by the Chinese Academy of Sciences through the Silk Road Project at NAOC, the President’s International Fellowship (PIFI) for Visiting Scientists program of CAS. The work of PB, MI and MS was also supported by the Volkswagen Foundation under the Trilateral Partnerships grants No. 90411 and 97778. This work has made use of

data from the European Space Agency (ESA) mission *GAIA* (<https://www.cosmos.esa.int/gaia>), processed by the *GAIA* Data Processing and Analysis Consortium (DPAC, <https://www.cosmos.esa.int/web/gaia/dpac/consortium>). Funding for the DPAC has been provided by national institutions, in particular the institutions participating in the *GAIA* Multilateral Agreement.

The authors is grateful to an anonymous referee for useful comments and suggestions that helped to improve the manuscript.

REFERENCES

- [1] Allen C., Moreno E., Pichardo B. 2006, *AJ*, 652, 2
- [2] Allen C., Moreno E., Pichardo B. 2008, *AJ*, 674, 1
- [3] Bajkova A.T., Bobylev V.V. *Astronomical and Astrophysical Transactions*, 2021, 32, 3, p. 177-206
- [4] Bajkova A.T., Bobylev V.V., 2021, *Research in Astronomy and Astrophysics*, 21, 173
- [5] Bastian N., Pfeffer J. 2021, accepted in *MNRAS*, eprint [arXiv:2110.10616](https://arxiv.org/abs/2110.10616)
- [6] Baumgardt H., Hilker M., Sollima A., Bellini A. 2019, *MNRAS*, 482, 4
- [7] Bennett M., Bovy J. 2019, *MNRAS*, 482, 1417
- [8] Berczik P., Nitadori K., Zhong S. et al. 2011, in *International conference on High Performance Computing*, Kyiv, Ukraine, p. 8-18
- [9] Chemerynska I.V., Ishchenko M.V., Sobolenko M.O., Khoperskov S.A., Berczik P.P., *Advances in Astronomy and Space Physics*, 2021, submitted
- [10] *Gaia* Collaboration: Helmi I., van Leeuwen F., McMillan P.J. et al. 2018, *A&A*, 616, A12
- [11] *Gravity* Collaboration: Abuter R., Amorim A., Bauböck M. et al. 2019, *A&A*, 625, L10
- [12] Gnedin O.Y., Ostriker J.P. 1997, *AJ*, 474, 1
- [13] Harfst S., Gualandris A., Merritt D. et al. 2007, *New Astron.*, 12, 357
- [14] Ibata R.A., Gilmore G., Irwin M.J. 1994, *Nature*, 370, 6486
- [15] Johnson D.R.H., Soderblom D.R. 1987, *AJ*, 93, 864
- [16] Kharchenko N.V., Piskunov A.E., Schilbach E., Röser S., Scholz R.D. 2013, *A&A*, 558, A53
- [17] Kruijssen J.M.D., Pfeffer J.L., Chevance M. et al. 2020, *MNRAS*, 498, 2
- [18] Mardini M.K., Placco V.M., Meiron Y. et al. 2020, *ApJ*, 903, 88
- [19] Massari D., Koppelman H.H., Helmi A. 2019, *A&A*, 630, L4
- [20] Miyamoto M., Nagai R. 1975, *Publications of the Astronomical Society of Japan*, 533-534, 27
- [21] Moreno E., Pichardo B., Velázquez H. 2014, *AJ*, 793, 2
- [22] Navarro J.F., Frenk C.S., White S.D.M. et al. 1997, *ApJ*, 490, 2
- [23] Pichardo B., Martos M., Moreno E. 2004, *AJ*, 609, 1
- [24] Pérez-Villegas A., Rossi L., Ortolani S. et al. 2018, *Publications of the Astronomical Society of Australia*, 35

- [25] Pérez-Villegas A., Barbuy B., Kerber L.O. et al. 2020, MNRAS, 491, 3
 [26] Schönrich R., Binney J, Dehnen W. 2010, MNRAS, 403, 4
 [27] Souza S.O., Valentini M., Barbuy B. et al. 2021, accepted in A&A, eprint [arXiv:2109.04483](https://arxiv.org/abs/2109.04483)
 [28] Vasiliev E. 2019, MNRAS, 484, 2

Table 4: Initial list of GCs.

ID	Name	Flag	ID	Name	Flag	ID	Name	Flag	ID	Name	Flag	ID	Name	Flag
1	NGC 104		32	NGC 5634		63	NGC 6273		94	Terzan 5		125	NGC 6656	
2	NGC 288		33	NGC 5694		64	NGC 6284		95	NGC 6440		126	Pal 8	
3	NGC 362		34	IC 4499		65	NGC 6287		96	NGC 6441		127	NGC 6681	
4	Whiting 1		35	NGC 5824		66	NGC 6293		97	Terzan 6		128	NGC 6712	bh
5	NGC 1261		36	Pal 5		67	NGC 6304		98	NGC 6453		129	NGC 6715	
6	Pal 1	me	37	NGC 5897		68	NGC 6316		99	NGC 6496		130	NGC 6717	
7	E 1	me	38	NGC 5904		69	NGC 6341		100	Terzan 9	bh	131	NGC 6723	
8	Eridanus		39	NGC 5927		70	NGC 6325		101	Djorg 2	cc	132	NGC 6749	
9	Pal 2		40	NGC 5946		71	NGC 6333		102	NGC 6517		133	NGC 6752	
10	NGC 1851		41	BH 176	me	72	NGC 6342		103	Terzan 10		134	NGC 6760	me
11	NGC 1904		42	NGC 5986		73	NGC 6356		104	NGC 6522	cc	135	NGC 6779	
12	NGC 2298		43	FSR 1716		74	NGC 6355	cc	105	NGC 6535		136	Terzan 7	
13	NGC 2419		44	Pal 14		75	NGC 6352		106	NGC 6528		137	Pal 10	
14	Pyxis		45	BH 184		76	IC 1257		107	NGC 6539		138	Arp 2	
15	NGC 2808		46	NGC 6093		77	Terzan 2		108	NGC 6540		139	NGC 6809	
16	E 3		47	NGC 6121	bh	78	NGC 6366		109	NGC 6544	bh	140	Terzan 8	
17	Pal 3	me	48	NGC 6101		79	Terzan 4		110	NGC 6541		141	Pal 11	
18	NGC 3201		49	NGC 6144		80	BH 229		111	ESO 280-6		142	NGC 6838	
19	Pal 4	me	50	NGC 6139		81*	FSR 1758		112	NGC 6553	cc	143	NGC 6864	
20	Crater		51	Terzan 3	cc	82	NGC 6362		113	NGC 6558		144	NGC 6934	
21	NGC 4147		52	NGC 6171		83*	Liller 1	cc, bh	114	Pal 7		145	NGC 6981	
22	NGC 4372		53	ESO 452-11	bh	84	NGC 6380		115	Terzan 12		146	NGC 7006	
23	Rup 106		54	NGC 6205		85	Terzan 1		116	NGC 6569		147	NGC 7078	
24	NGC 4590		55	NGC 6229		86	Ton 2		117	BH 261		148	NGC 7089	
25	NGC 4833		56	NGC 6218	cc	87	NGC 6388		118	NGC 6584		149	NGC 7099	
26	NGC 5024		57	FSR 1735	me	88	NGC 6402		119	NGC 6624		150	Pal 12	
27	NGC 5053		58	NGC 6235		89	NGC 6401		120	NGC 6626		151	Pal 13	
28	NGC 5139		59	NGC 6254		90	NGC 6397		121	NGC 6638	bh	152	NGC 7492	
29	NGC 5272		60	NGC 6256		91	Pal 6	bh	122	NGC 6637	cc, bh			
30	NGC 5286	me	61	Pal 15		92	NGC 6426		123	NGC 6642	bh			
31	NGC 5466		62	NGC 6266		93	Djorg 1		124	NGC 6652	bh			

NOTE: Parameters for all GCs was taken from [28] with the exception for GCs marked * with data from [6]. Column Flag contains additional information: me - GC excluded from the integration due to their significant measurement errors, cc - GC satisfied "collision" conditions, bh - GC interacted with central Black Hole.

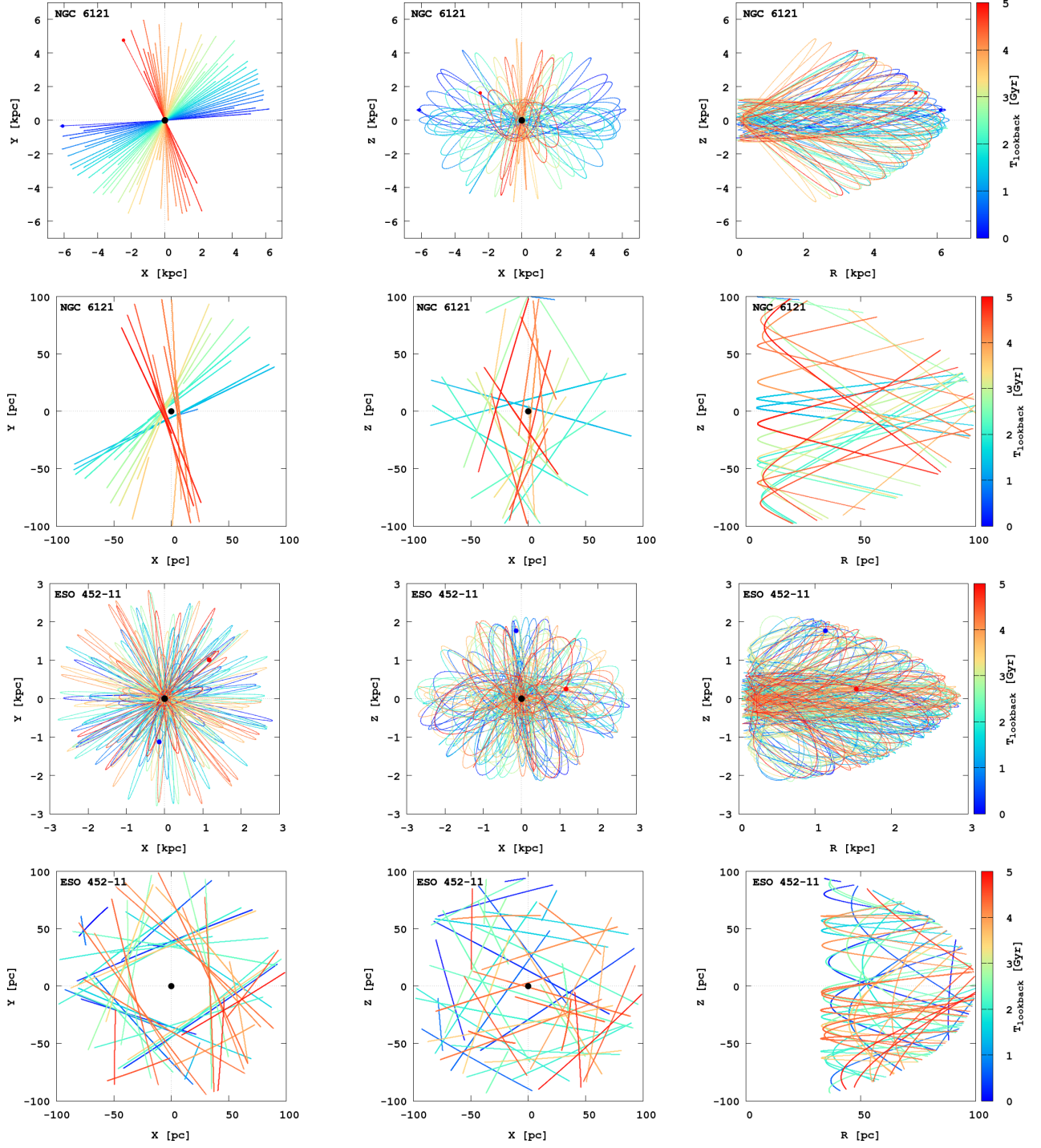


Fig. 4: GC NGC 6121 and ESO 452-11 (from top to bottom) orbits in $X - Y$ plane (left), in $X - Z$ plane (middle) and in $Z - R$ plane (right), where R is distance in the Galactic plane.

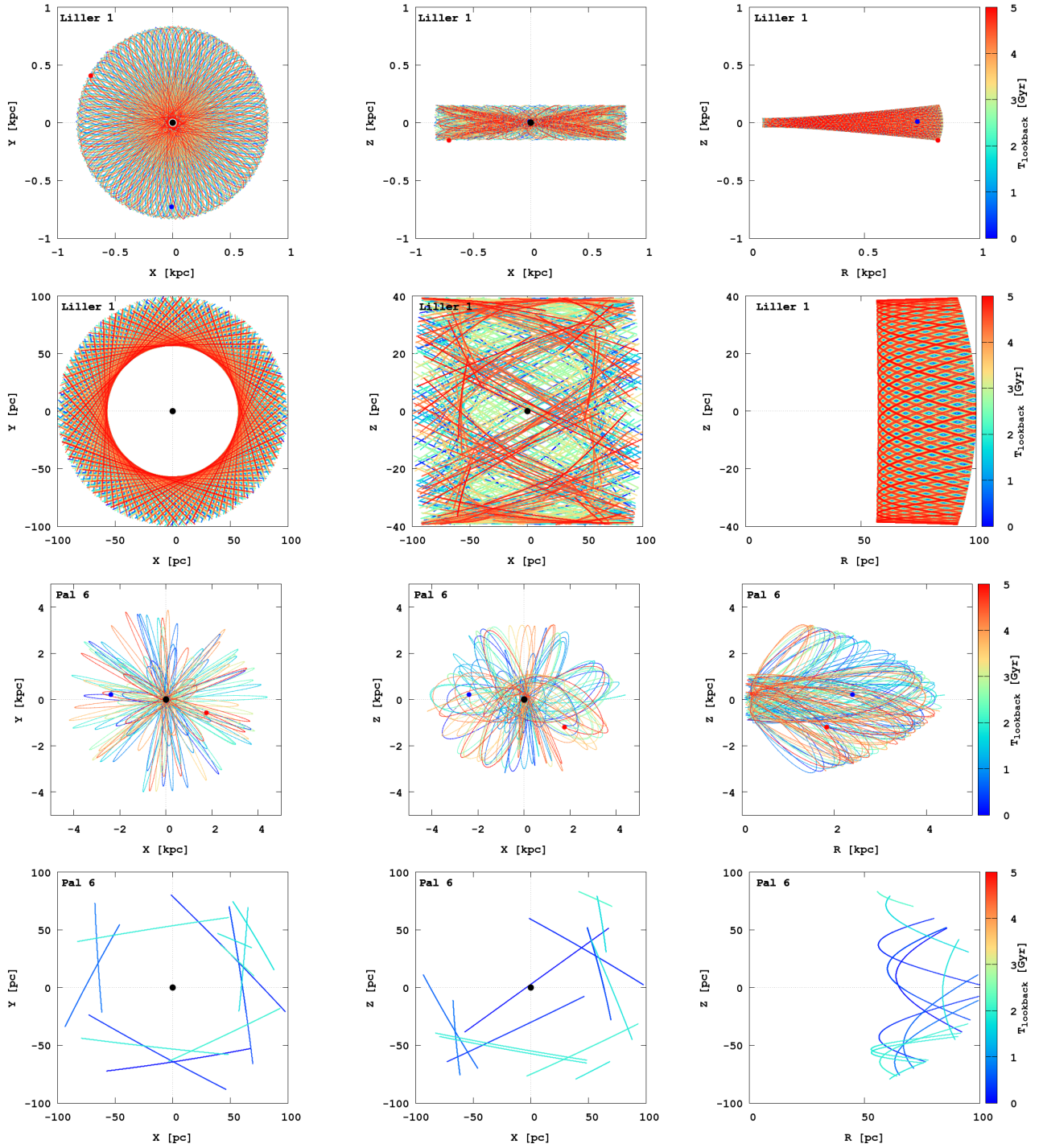


Fig. 5: As in Fig. 4 for Liller 1 and Pal 6.

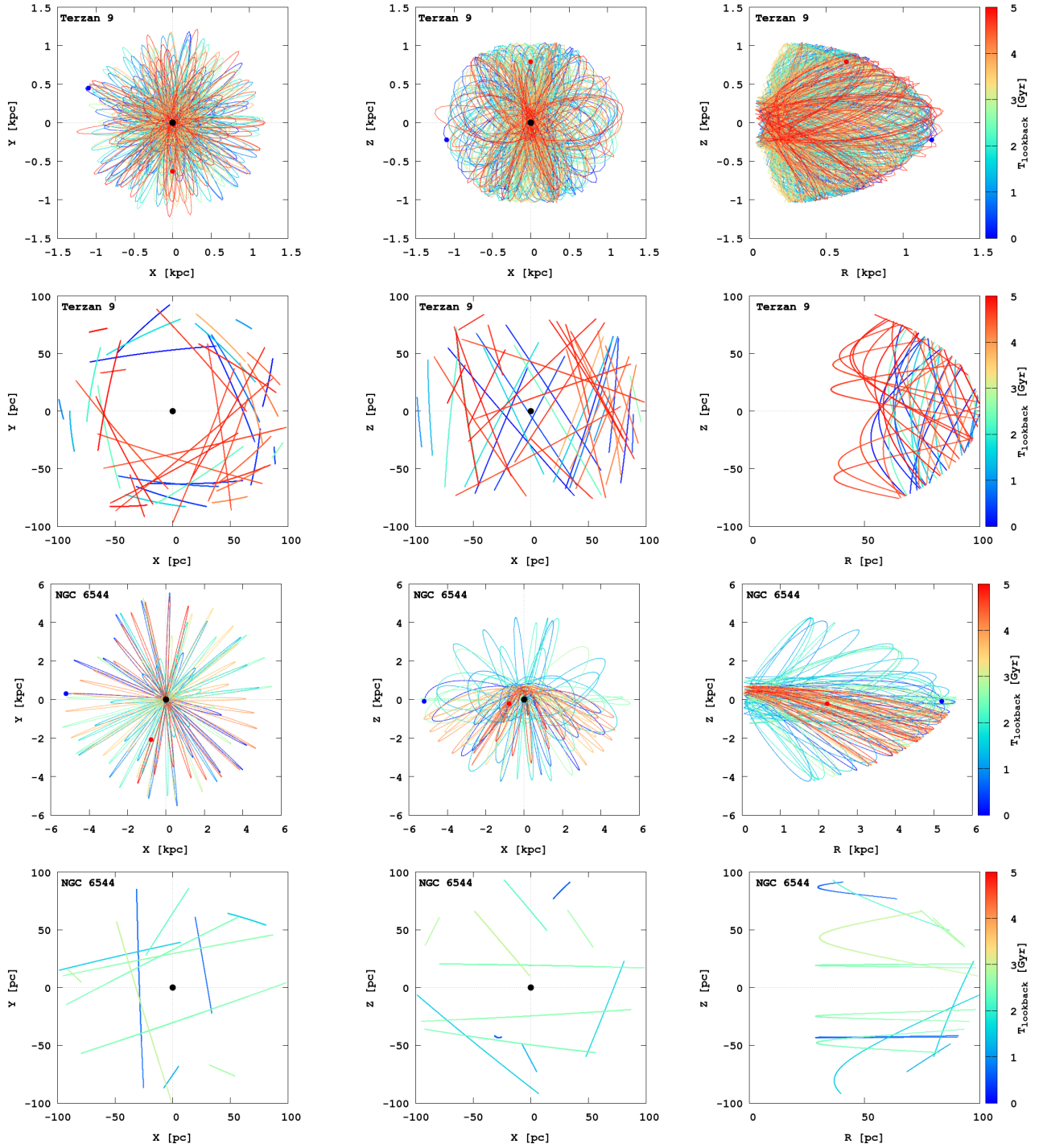


Fig. 6: As in Fig. 4 for Terzan 9 and NGC 6544.

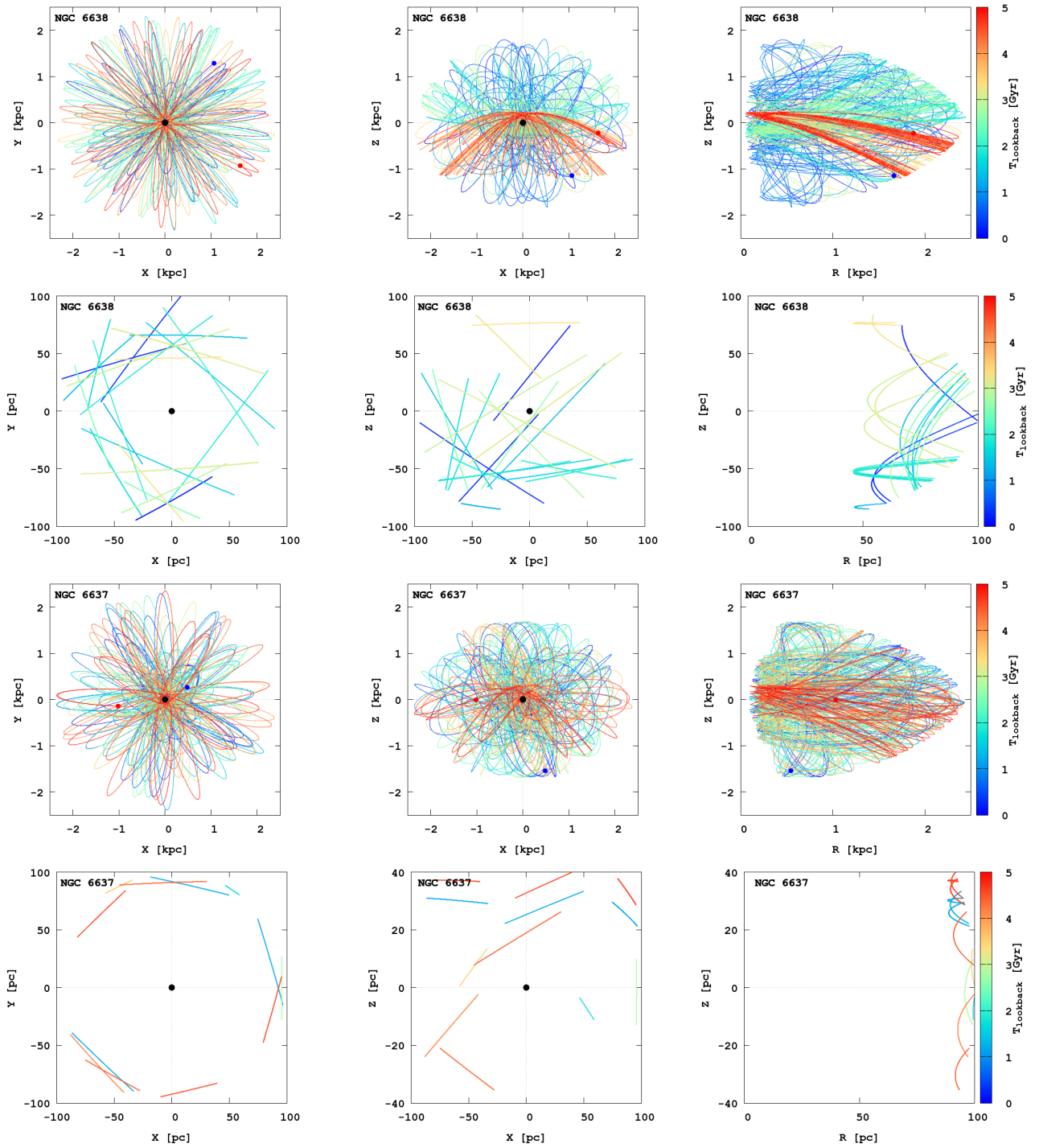


Fig. 7: As in Fig. 4 for NGC 6638 and NGC 6637.

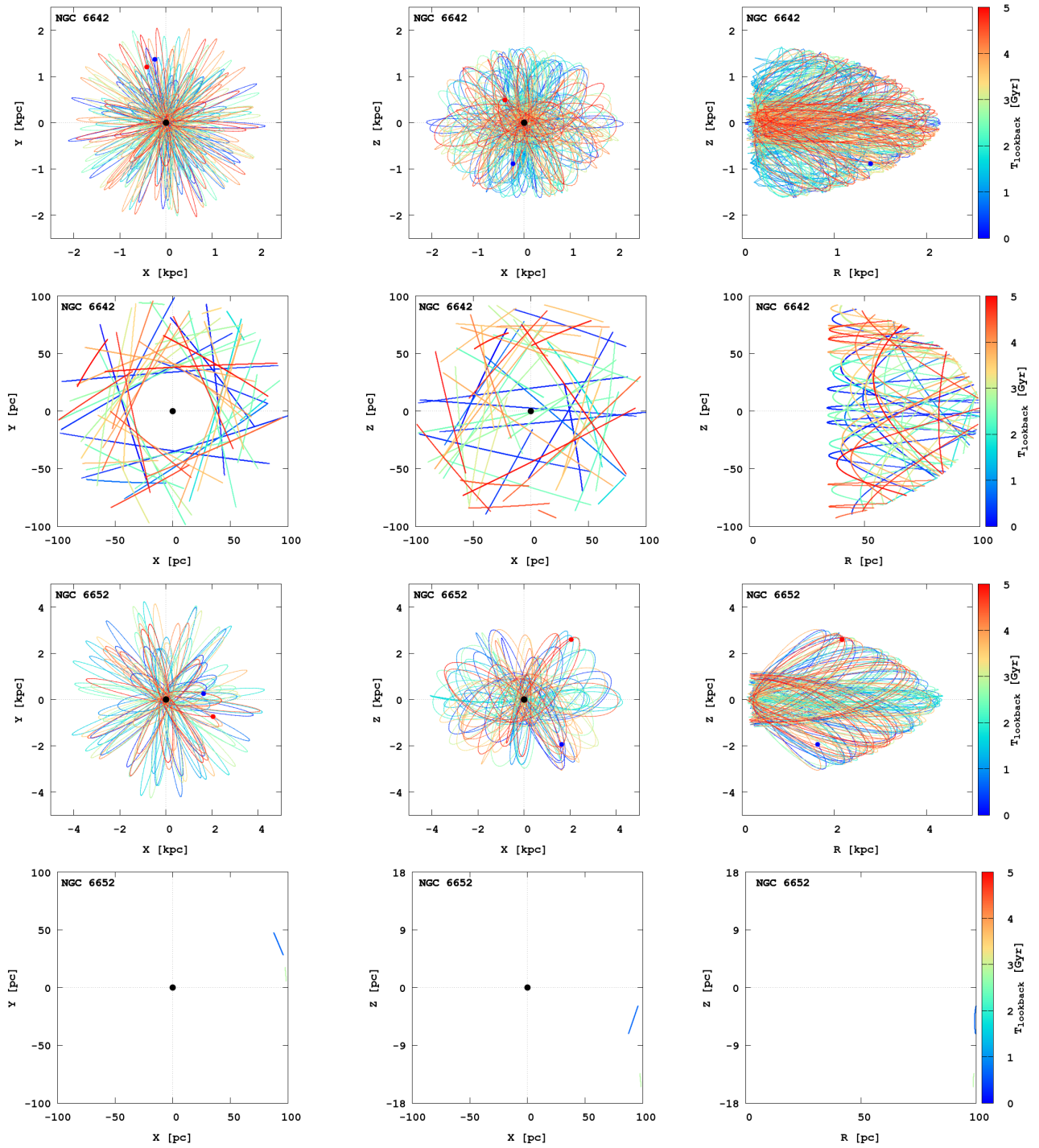


Fig. 8: As in Fig. 4 for NGC 6642 and NGC 6652.

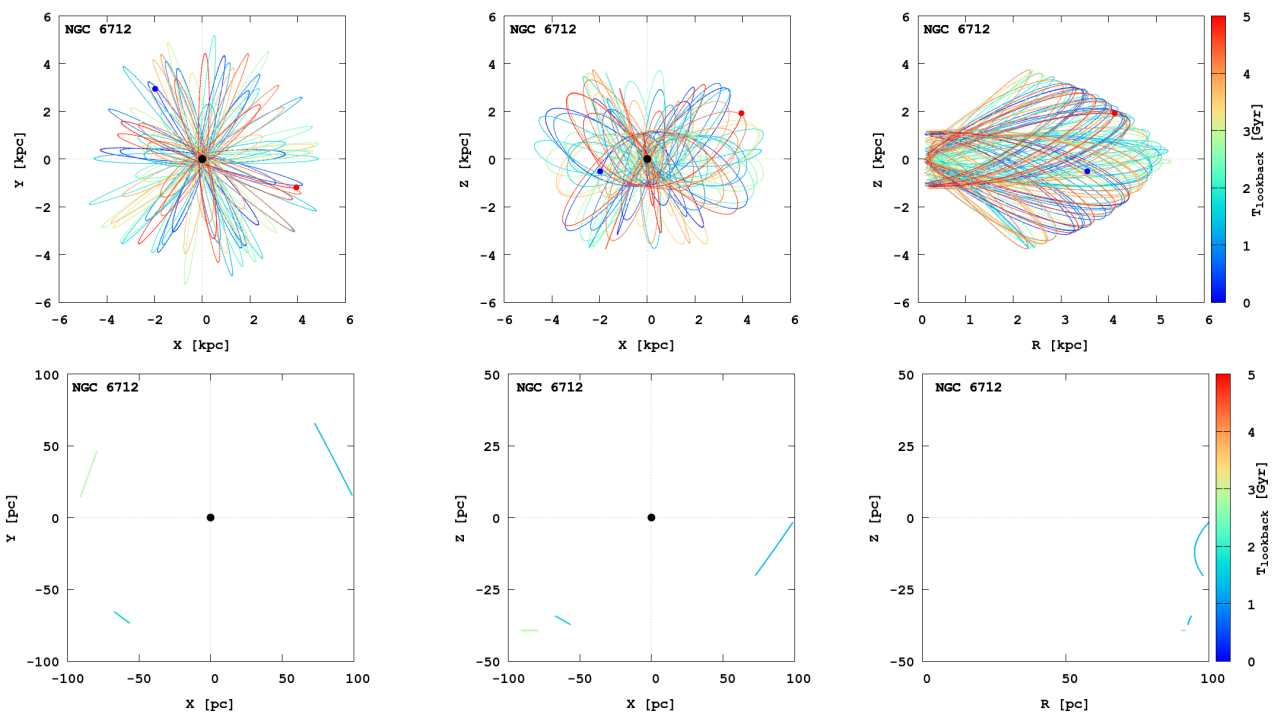


Fig. 9: As in Fig. 4 for NGC 6712.